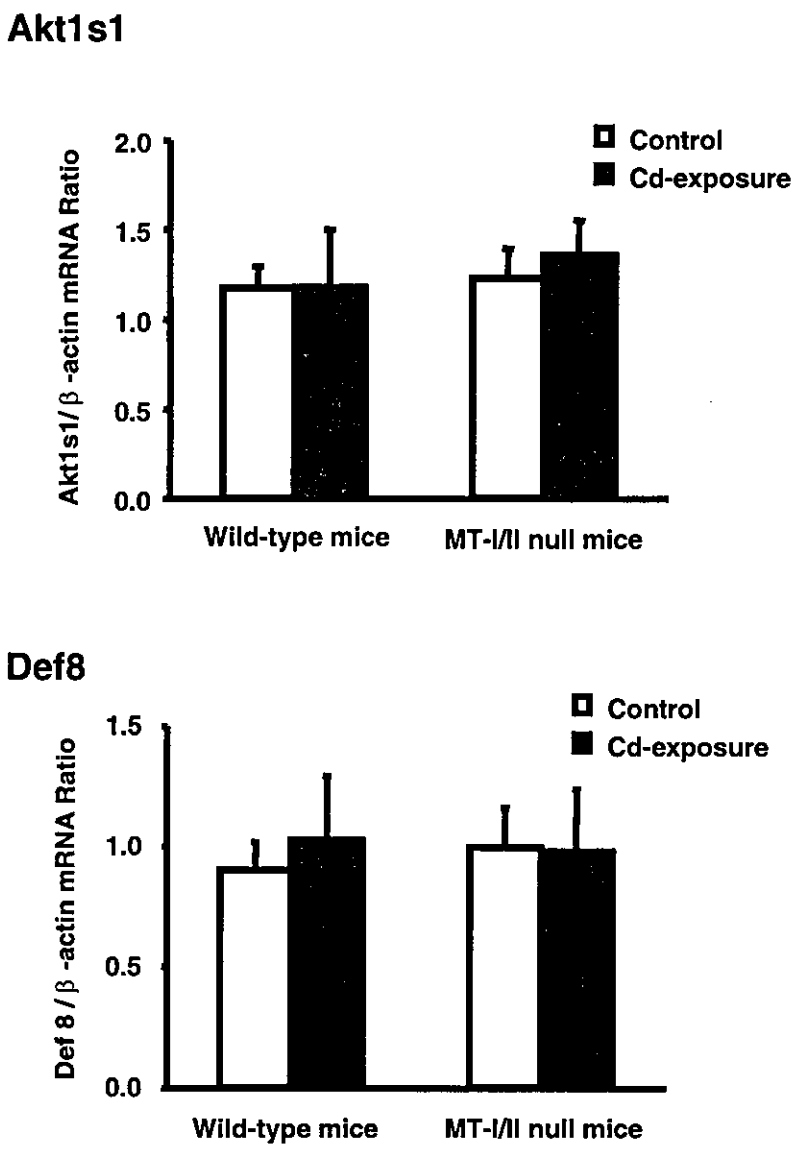

Fig. 7 Expression of Akt1s1 [matrix protein (ma), p15 containing protein data source:pfam, source key:pf01140, evidence:iss putative] and Def8 [expressed sequence ai449518] genes in neonatal brain of wild-type mice and MT-I/II null mice exposed to cadmium during gestation and lactation

Real-time RT-PCR analysis was performed on Akt1s1 and Def8 genes.

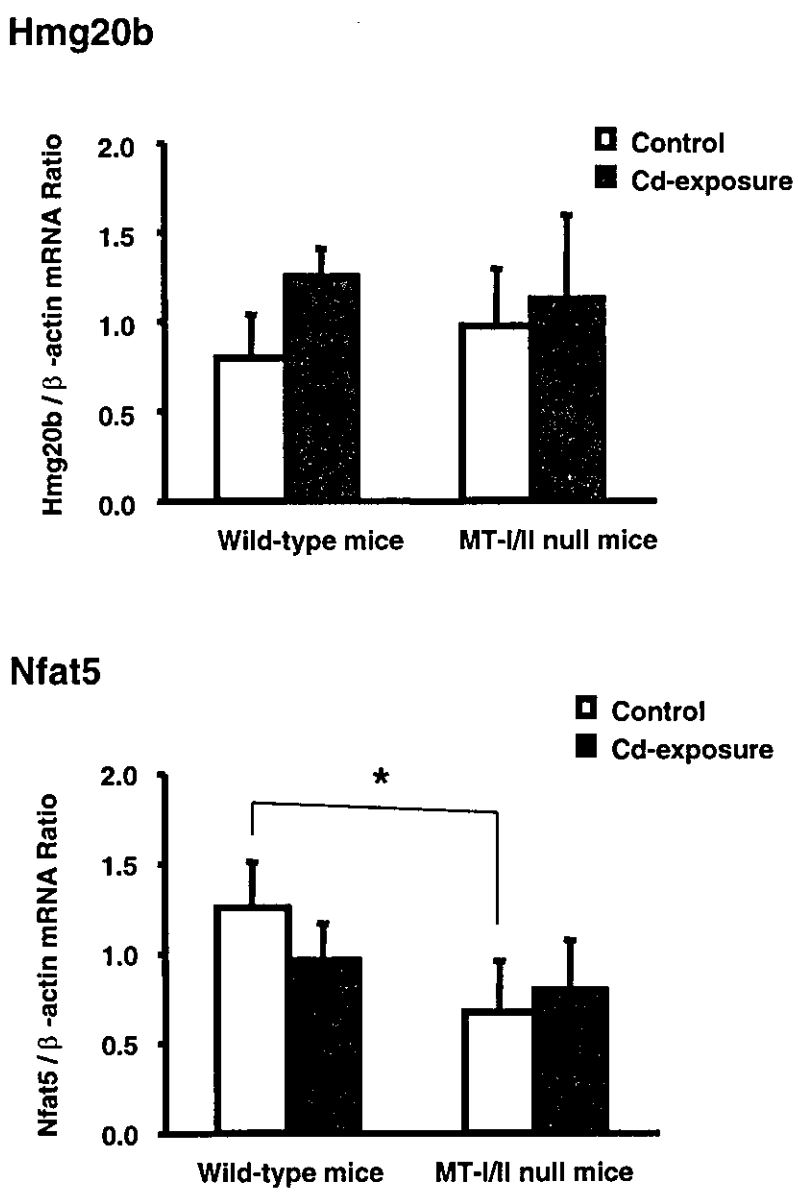

Fig. 8 Expression of Hmg20b [high mobility group protein 20 b] and Nfat5 [nuclear factor of activated t-cells 5] genes in neonatal brain of wild-type mice and MT-I/II null mice exposed to cadmium during gestation and lactation

Real-time RT-PCR analysis was performed on Hmg20b and Nfat5 genes. *P<0.05.

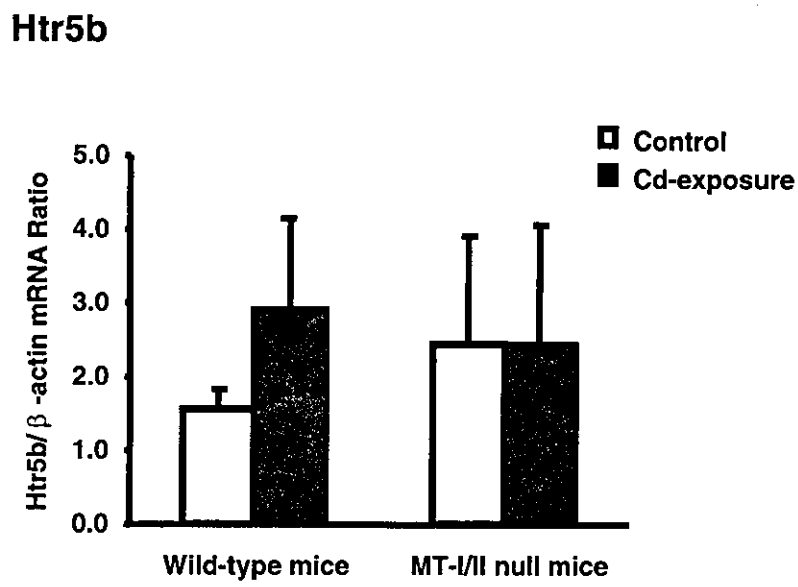

Fig. 9 Expression of Htr5b [5-hydroxytryptamine (serotonin) receptor 5b] gene in neonatal brain of wild-type mice and MT-I/II null mice exposed to cadmium during gestation and lactation

Real-time RT-PCR analysis was performed on Htr5b gene.

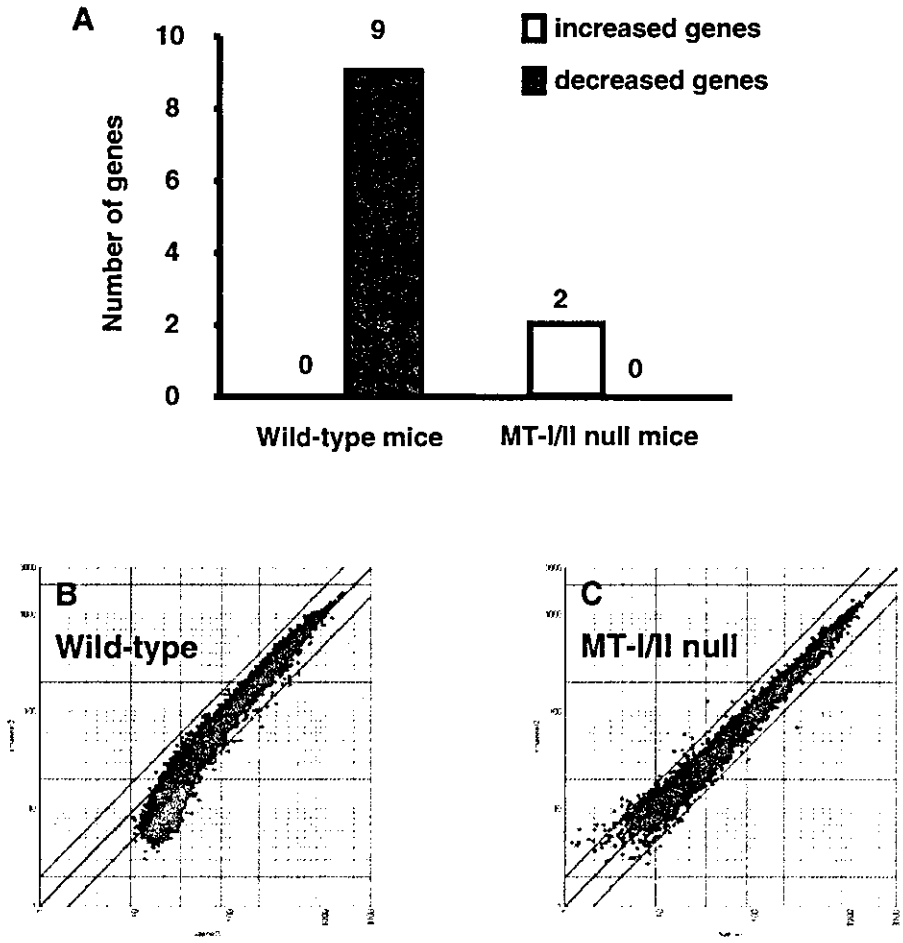

Fig. 10 Gene expression altered by methyl mercury exposure in neonatal brain of wild-type mice and MT-I/II null mice from microarray data
A : Number of genes altered by methyl mercury exposure in wild-type mice and MT-I/II null mice.
B : Scatter plot of control group (Cy3) of wild-type mice vs MeHg-exposure group (Cy5) of wild-type mice fluorescence intensity signal for each gene.
C : Scatter plot of control group (Cy3) of MT-I/II null mice vs MeHg-exposure group (Cy5) of MT-I/II null mice fluorescence intensity signal for each gene.

X-axis : Control group (Cy3), Y-axis : MeHg-exposure group (Cy5).

Table 5 Altered gene expression from microarray data of control group (Cy3) of wild-type mice vs MeHg-exposure group (Cy5) of wild-type mice hybridization

Gene Description	Ratio
Wild-type (MeHg-exposure) / Wild-type (Control) ≥ 2	
None	
Wild-type (MeHg-exposure) / Wild-type (Control) <0.5	
RPL32 [ribosomal protein l32]	0.38
Akt1s1 [matrix protein (ma), p15 containing protein data source:pfam, source key:pf01140, evidence:iss putative]	0.39
RPS12 [ribosomal protein s12]	0.43
RPS20 [ribosomal protein s20]	0.44
PLP [6.8 kda mitochondrial proteolipid]	0.45
RPL38 [ribosomal protein L38]	0.46
Nme2 [expressed in non-metastatic cells 2, protein (nm23b)]	0.47
RPS29 [ribosomal protein s29]	0.48
Cox7b [cytochrome c oxidase subunit viib]	0.50

Table 6 Altered gene expression from microarray data of control group (Cy3) of MT-I/II null mice vs MeHg-exposure group (Cy5) of MT-I/II null mice hybridization

Gene Description	Ratio
MT-I/II null (MeHg-exposure) / MT-I/II null (Control) ≥ 2	
Xist [nuclear-localized inactive x-specific transcript]	4.0
TIMP4 [tissue inhibitor of metalloproteinase 4]	2.2
MT-I/II null (MeHg-exposure) / MT-I/II null (Control) <0.5	
None	

Akt1s1

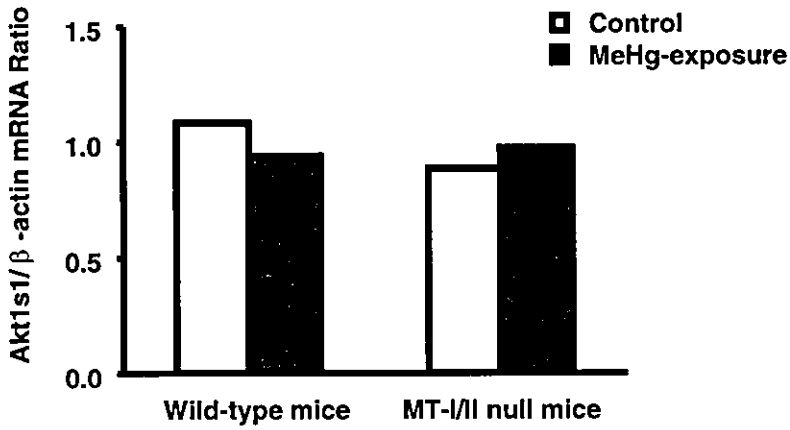

RPS12

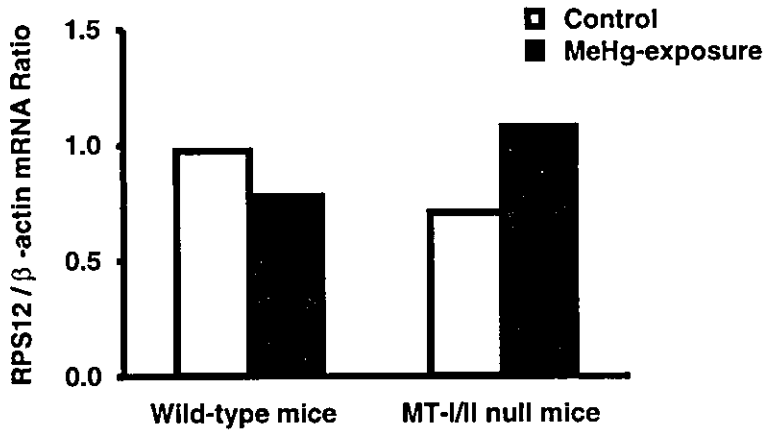

Fig. 11 Expression of Akt1s1 [matrix protein (ma), p15 containing protein data source:pfam, source key:pf01140, evidence:iss putative] and RPS12 [ribosomal protein s12] genes in neonatal brain of wild-type mice and MT-I/II null mice exposed to methyl mercury during gestation and lactation

Real-time RT-PCR analysis was performed on Akt1s1 and RPS12 genes.

PLP

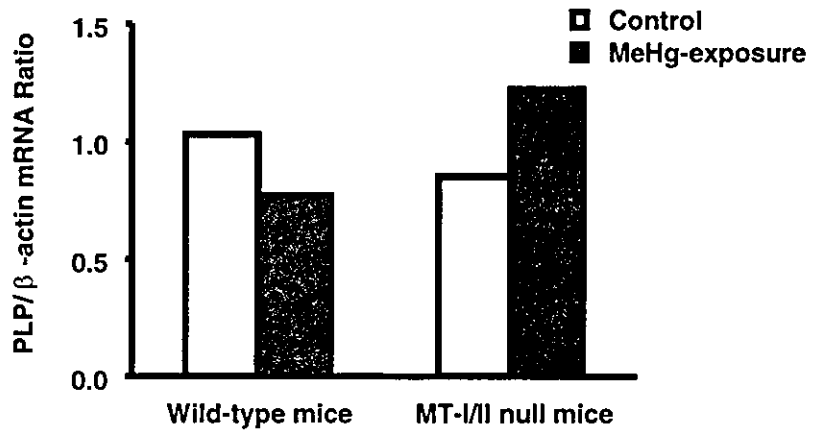

RPS20

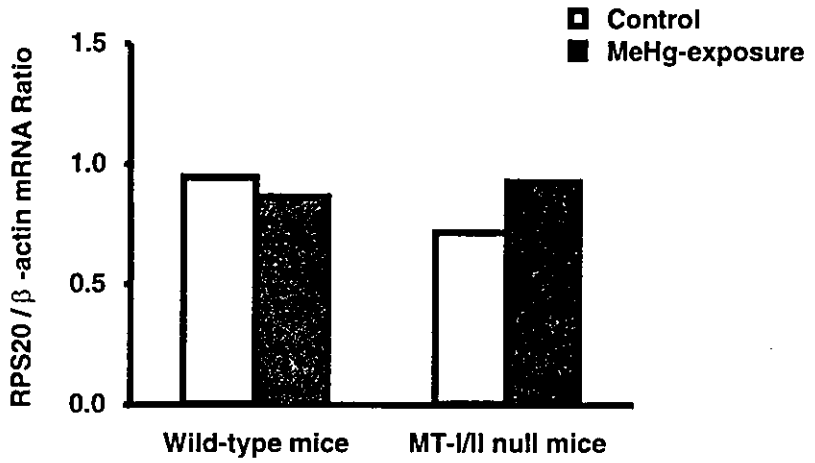

Fig. 12 Expression of PLP [6.8 kda mitochondrial proteolipid] and RPS20 [ribosomal protein s20] genes in neonatal brain of wild-type mice and MT-I/II null mice exposed to methyl mercury during gestation and lactation

Real-time RT-PCR analysis was performed on PLP and RPS20 genes.

RPL38

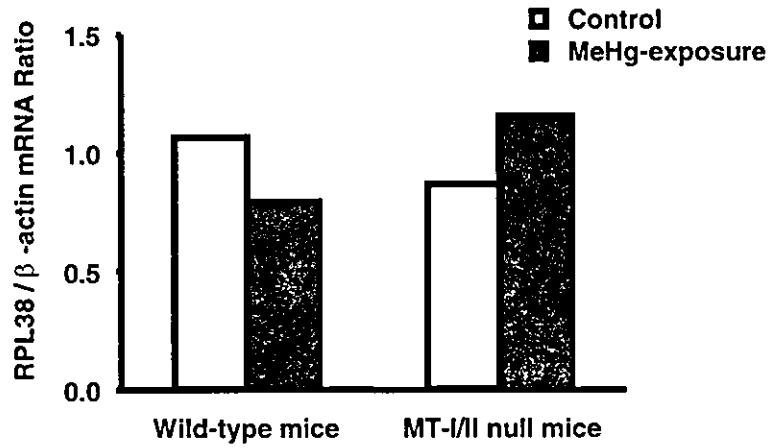

Nme2

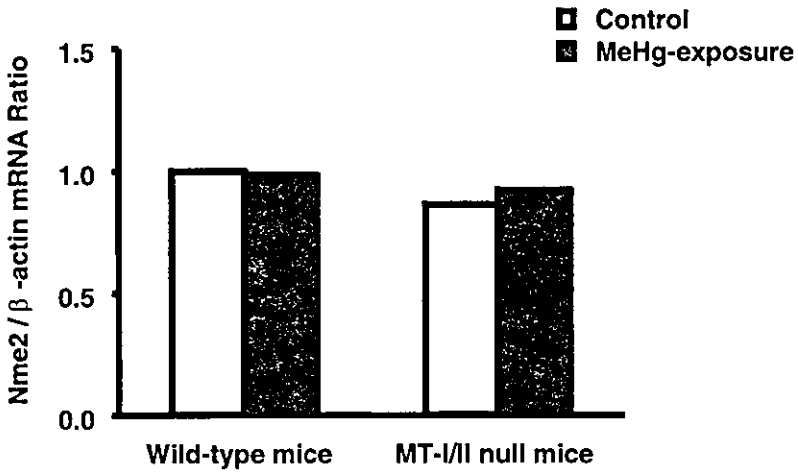

Fig. 13 Expression of RPL38 [ribosomal protein L38] and Nme2 [expressed in non-metastatic cells 2, protein (nm23b)] genes in neonatal brain of wild-type mice and MT-I/II null mice exposed to methyl mercury during gestation and lactation

Real-time RT-PCR analysis was performed on RPL38 and Nme2 genes.

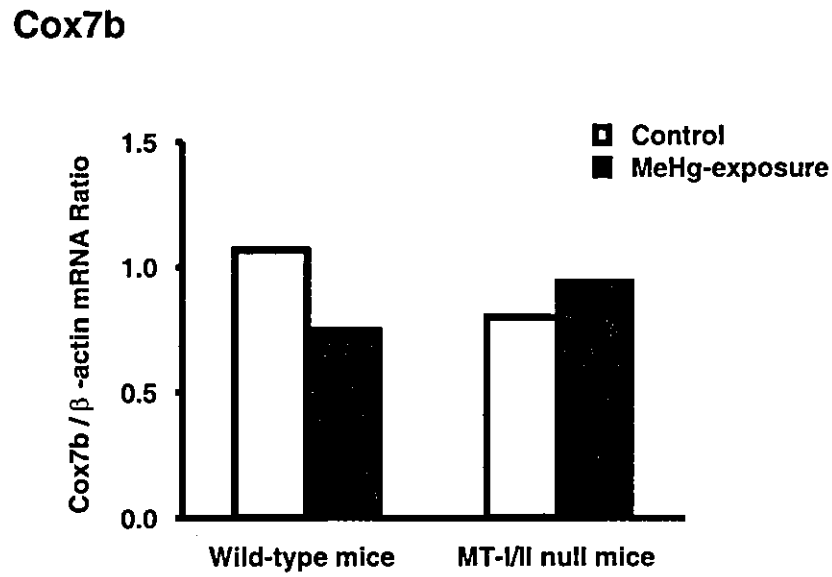

Fig. 14 Expression of Cox7b [cytochrome c oxidase subunit viib] gene in neonatal brain of wild-type mice and MT-I/II null mice exposed to methyl mercury during gestation and lactation

Real-time RT-PCR analysis was performed on Cox7b gene.

Xist

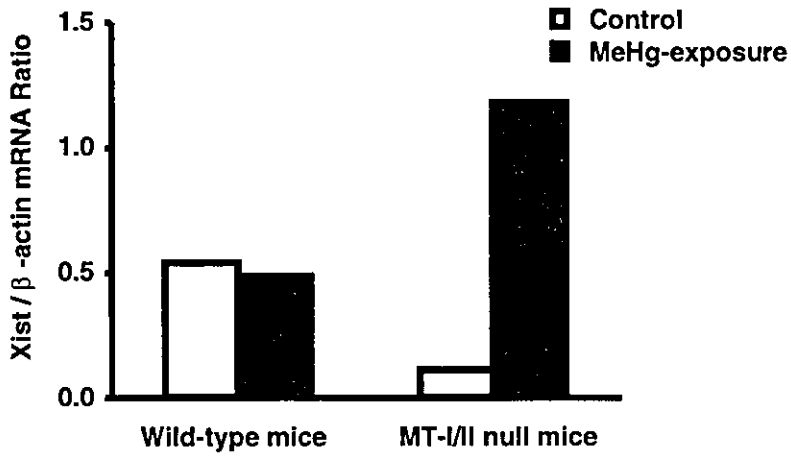

TIMP4

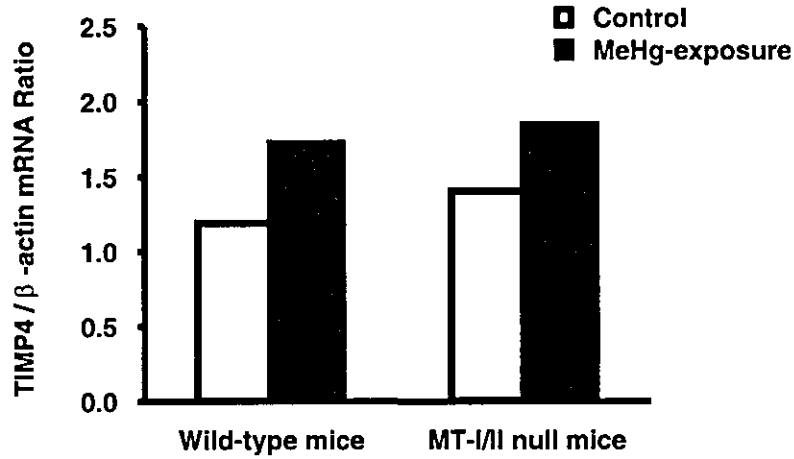

Fig. 15 Expression of Xist [nuclear-localized in active x-specific transcript] and TIMP4 [tissue inhibitor of metalloproteinase 4] genes in neonatal brain of wild-type mice and MT-I/II null mice exposed to methyl mercury during gestation and lactation

Real-time RT-PCR analysis was performed on Xist and TIMP4 genes.

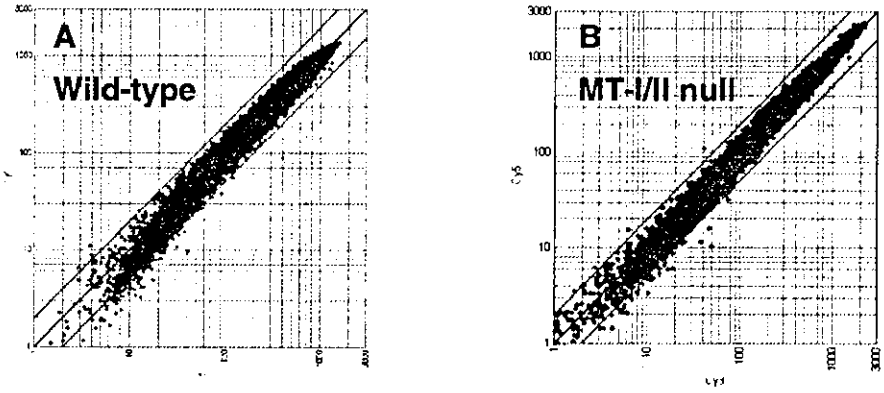

Fig. 16 Gene expression altered by methyl mercury exposure in brain of wild-type mice and MT-I/II null mice from microarray data
A : Scatter plot of control group (Cy3) of wild-type mice vs MeHg-exposure group (Cy5) of wild-type mice fluorescence intensity signal for each gene.
B : Scatter plot of control group (Cy3) of MT-I/II null mice vs MeHg-exposure group (Cy5) of MT-I/II null mice fluorescence intensity signal for each gene.

X-axis : Control group (Cy3), Y-axis : MeHg-exposure group (Cy5).

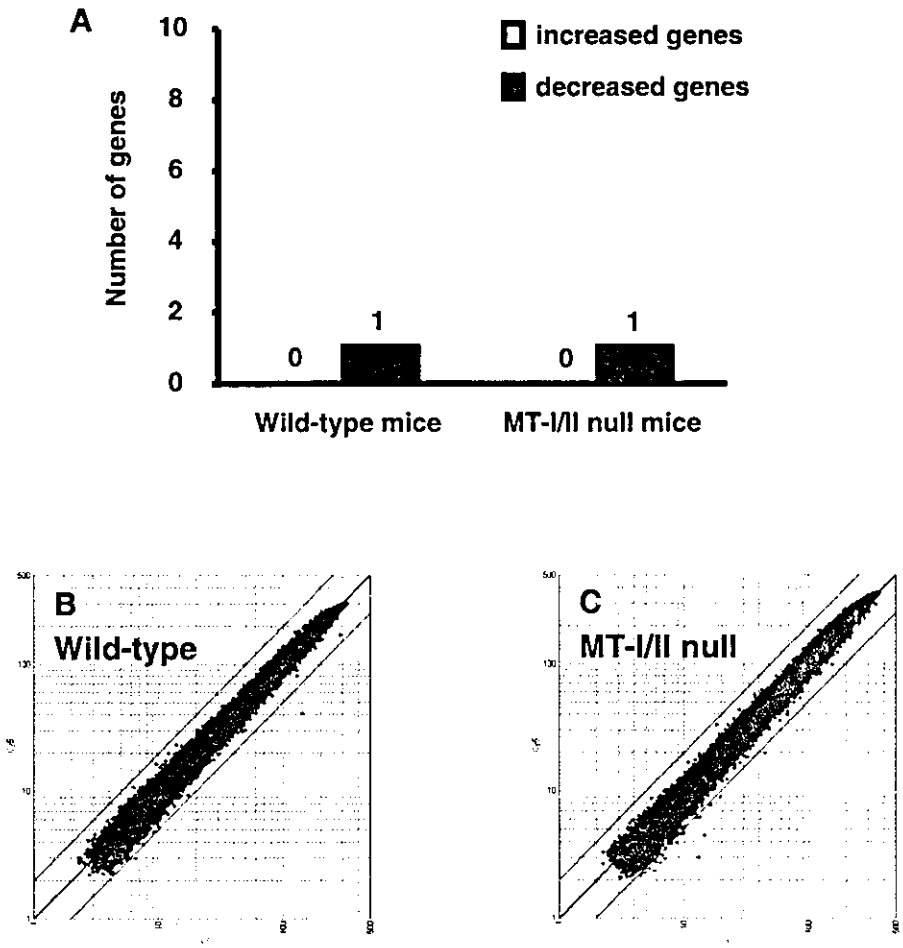

Fig. 17 Gene expression altered by combined exposure to methyl mercury and mercury vapor in neonatal brain of wild-type mice and MT-I/II null mice from microarray data

A : Number of genes altered by combined exposure to methyl mercury and mercury vapor in wild-type mice and MT-I/II null mice.

B : Scatter plot of control group (Cy3) of wild-type mice vs MeHg+Hg^0 -exposure group (Cy5) of wild-type mice fluorescence intensity signal for each gene.

C : Scatter plot of control group (Cy3) of MT-I/II null mice vs MeHg+Hg^0 -exposure group (Cy5) of MT-I/II null mice fluorescence intensity signal for each gene.

X-axis : Control group (Cy3), Y-axis : MeHg+Hg^0 -exposure group (Cy5).

Table 7 Altered gene expression from microarray data of control group (Cy3) of wild-type mice vs MeHg+Hg^0 -exposure group (Cy5) of wild-type mice hybridization

Gene Description	Ratio
Wild-type (MeHg+Hg^0-exposure) / Wild-type (Control) $>$ 2	
Masp2 [mannan-binding lectin serine protease 2]	0.28
Wild-type (MeHg+Hg^0-exposure) / Wild-type (Control) $<$ 0.5	
None	

Table 8 Altered gene expression from microarray data of control group (Cy3) of MT-I/II null mice vs MeHg+Hg^0 -exposure group (Cy5) of MT-I/II null mice hybridization

Gene Description	Ratio
MT-I/II null (MeHg+Hg^0) / MT-I/II null (Control) $>$ 2	
None	
MT-I/II null (MeHg+Hg^0) / MT-I/II null (Control) $<$ 0.5	
ENSMUST00000041202 acetolactate synthase [source:ensembl_protein_families;acc:ensmusf00000004722]; acetolactate synthase	0.44

厚生労働科学研究費補助金（化学物質リスク研究事業）
分担研究報告

Time dependent changes of mercury distribution in the murine spinal cord after exposure to low concentration mercury vapor

低濃度水銀蒸気曝露マウスにおける脊髄内の水銀顆粒沈着部位の経時的変化

分担研究者　島田章則　鳥取大学農学部獣医病理学教授

研究要旨

本プロジェクトでは水銀蒸気曝露を、メチル水銀毒性の修飾要因ととらえ、その影響を検討してきたが、その過程において水銀蒸気の神経系における輸送にこれまで知られていない経路が関与している可能性を指摘した。本研究では、この点について低濃度（0.04ー0.1mg／m^3）水銀蒸気曝露における脊髄への水銀分布を４週間にわたり経時的に追跡することによって検討した。その結果、脊髄への侵入には逆行性軸策輸送が使われていること、脊髄内の移動には transneuronal な（神経細胞から神経細胞への）経路も使用されていることが示唆された。

ABSTRACT

The central nervous system (CNS) is the critical organ for elemental (metallic) mercury (Hg^0) exposure. Over-exposure to mercury vapor gives rise to neurological effects and neurobehavioral impairment. Until now, there are

many studies related to transport pathway to the CNS by inorganic mercury, but studies which related to the transport pathway in the CNS are not performed. Therefore, this study was performed to examine effects and time dependent mercury distribution in the spinal cord caused by low concentration exposure to Hg^0 vapor by histopathological references, and then, to hypothesis the transport pathway of mercury to and in the spinal cord according to the mercury distributions. Sixteen mice were exposed to Hg^0 vapor (0.040 to 0.100 mg/m^3) all day for 1, 3, 7, 10, 14, 21 and 28 days. Mice were killed under diethylether anesthesia after exposure. The spinal cord was taken from each mouse. Histopathological examinations including autometallography, and double staining for immunohistocemistry (GFAP) and autometallography, for mercury distribution were performed. No histopathological changes were seen in the spinal cord. No mercury were seen in sections obtained from control animals. Mercury deposits, which can be seen by light microscopy as black granules, were found to accumulate within neuronal perikarya of the neurons and astrocytes. Mercury granules were demonstrated in the all spinal cord sections examined. The mercury deposits were first detected in the motor neurons in ventral horn and spread out the neurons in the dorsal horn following to substancia intermedia. No mercury granules were seen in the endothelial cells of blood vessels in any areas of the spinal cord. By electron microscopy, mercury granules like substances were found in lysosome like structures of neurons and astrocytes. In conclusion, this study indicated that the transport pathway of the inorganic mercury to the spinal cord was suspected to retrograde axonal transport as same as studies previously performed. Furthermore, it was suggested that

transneuronal transport was one of the ways of mercury granules spread within the spinal cord.

INTRODUCTION

Elemental (metallic) mercury (Hg^0) is one of the inorganic mercury and a highly toxic metal that can cause serious adverse health effect [12]. Elemental mercury is generally recognized as a heavy, silver liquid at room temperature, and is found in thermometers, fluorescent light bulbs, barometers, manometers and switches in children's shoes that light up [12]. One environmental problem of concern today is occupational exposure to Hg^0 vapor occurs in a variety of industries, but the general population is primarily exposed from continuous off-gassing from dental amalgam fillings [8, 9, 12, 31].

The central nervous system (CNS) is the critical organ for Hg^0 vapor exposure [12]. Over-exposure to mercury vapor gives rise to neurological effects with initially a fine high-frequency intention tremor and neurobehavioral impairment [12]. Peripheral nerve involvement has also been observed [12]. Long-term, low-level exposure has been found to be associated with less pronounced symptoms of erethism, characterized by fatigue, irritability, loss of memory, vivid dreams and depression [12]. Despite these clinical observations, histological changes of low concentration Hg^0 vapor exposure on the CNS are not well understood.

In previous studies, two transport pathways of the inorganic mercury to the CNS have been reported. One is that inorganic mercury is transported by

bloodstream to the CNS [10, 11, 17-19, 28, 32, 33]. The details of system are that elementary mercury (Hg^0) readily crosses the lung alveoli due to its high difusibility and lipid solubility and is taken up by erythrocytes, in which catalases oxidize the elemental mercury to divalent ionic mercury (Hg^{2+}). Although the ionic mercury does not readily pass through the blood-brain barrier, a fraction of the metallic mercury is transferred from the bloodstream into tissues, including the CNS, where it is trapped by oxidation [17, 18, 28]. The other is that inorganic mercury is transported by retrograde axonal transport pathway to the CNS [1-5, 13, 21, 22, 27]. The system is that inorganic mercury (Hg^{2+}) is taken up in nerve terminals in skeletal muscles (neuromuscular junction) and then transported retrogradely along the motor neurons to the cell bodies in the spinal cord and dorsal root ganglia [3-5, 13, 27]. However, the details of the mechanism by which mercury is taken up at the nerve endings are not known [2].

Until now, there are many studies related to transport pathway to the CNS by inorganic mercury, but studies to the transport pathway within the CNS are not performed. Therefore, this study was performed to examine effects and time dependent mercury distribution in the spinal cord caused by low concentration exposure to Hg^0 vapor by histopathological references, and then, to suspect the transport pathway of mercury to and within the spinal cord according to the mercury distribution.

MATERIALS AND METHODS

Animals

Female C57BL/6J mice (4 weeks old) were obtained from Nippon Clea Co.

(Osaka, Japan). The animal facility was maintained under temperature of 23 ±1℃, relative humidity of 55±10%, and negative atmospheric pressure. The mice received mouse chow and filtered tap water *ad libitum*.

Exposure to mercury (Hg^0) vapor (For light microscopy)

Experimental groups were exposed to Hg^0 vapor (0.040 to 0.100 mg/m^3) all day for period of 1, 3, 7, 10, 14, 21,and 28 days (Table. 1). Exposure system is shown in Fig. 1. Mercury concentration in the exposure chamber (20 liter) was measured once at 20 min by the air sampling method [13]. Control mice were exposed to mercury- free room air for 28 days before being sacrifices. Mice were killed under diethylether anesthesia after exposure to mercury vapor. Tissues for histological examination (spinal cord) were fixed in 10% neutral buffered formalin.

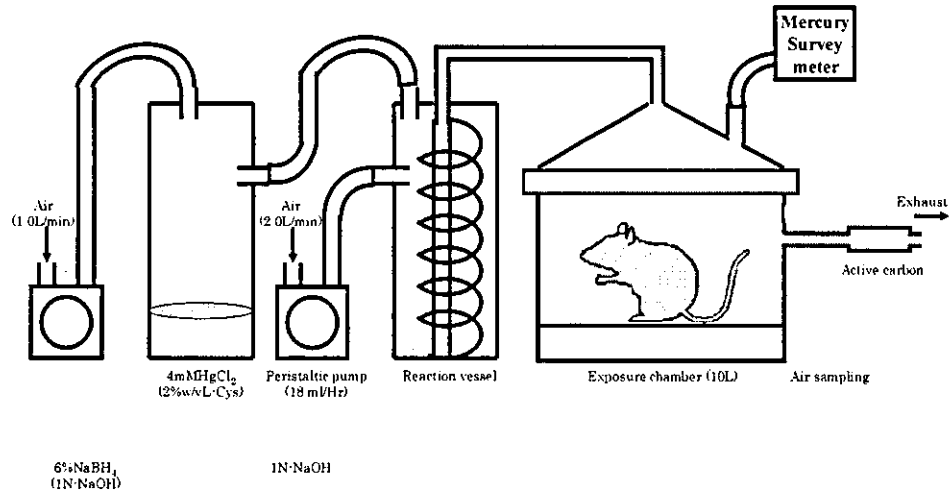

Fig. 1. Mercury vapor exposure system

Exposure to mercury (Hg^0) vapor (For electron microscopy)

Experimental groups were exposed to Hg^0 vapor (0.040 to 0.100 mg/m^3) all day for period of 7, 10 and 14 days. Exposure system is shown in Fig. 1. Mercury concentration in the exposure chamber (20 liter) was measured once at 20 min by the air sampling method [13]. Control mice were exposed to mercury- free room air before being sacrifices. Mice were killed under diethylether anesthesia by transcardial perfusion at 4 % paraformaldehyde in 0.1 M phosphate buffer (pH = 7.4) at room temperature. The spinal cords were removed and post-fixed in the same fixative for 12 h.

Table. 1 Experimental procedure

	n	Hg^0 vapor level (mg/m^3)	Exposure time (hour)	Duration of exposure (day)
Exposure	2	0.040-0.100	24	1
	2	0.040-0.100	24	3
	2	0.040-0.100	24	7
	2	0.040-0.100	24	10
	2	0.040-0.100	24	14
	2	0.040-0.100	24	21
	2	0.040-0.100	24	28
Control	2	0	0	0

Tissues: spinal cord

Histopathology

Tissues fixed in 10% neutral buffered formalin were embedded in paraffin, sectioned at 3 μ m and stained with hematoxylin and eosin (HE).

Autometallography

Paraffin sections were stained for mercury by autometallography [7]. The sections were pretreated with 1% potassium cyanide for 2h to eliminate non-specific staining from silver sulphides or selenides, placed in physical developer containing 50% gum Arabic, citrate buffer, hydroquinone and silver nitrate at 26℃ for 43 min in the dark. Excess silver was removed by 5% sodium thiosulphate. The sections were counterstained with hematoxylin. The reaction product was seen as small black grains of silver surrounding an invisible mercury core within the tissue.

Immunohistochemistry and Autometallography

The primary antibody used in this study was Glial Fibrillery Acidic Protein (GFAP) (N1506): (DakoCytomation, Inc., California, USA). Immunohistochemistry was performed on 3 μm paraffin section which was fixed with 10% neutral buffered formalin. Immunohistochemistry was performed by the avian-biotin peroxidase complex (ABC) method, in which labeled Streptavidin biotin (LSAB) kit (DAKO, Glostrup, Denmark) was included. After deparaffinization of the sections, to improve the binding of several antibodies, the sections were transferred into citric acid buffer and boiled for 20 minutes (min) at 98 ℃ in a micro oven according to a standard microwave treatment protocol. After blocking endogenous peroxidase activity with 3% H_2O_2, sections were preincubated with 10% normal goat serum for 5 min in the micro oven. Thereafter the sections were incubated with the respective primary antibody 10 min in the micro oven. The sections were sequentially incubated with peroxidase-conjugated goat anti-rabbit IgG diluted